Terahertz electron distribution modulation in piezoelectric $In_xGa_{1-x}N/GaN$ multiple quantum wells using coherent acoustic nanowaves

Kung-Hsuan Lin, Gia-Wei Chern, Yue-Kai Huang, and Chi-Kuang Sun*
Graduate Institute of Electro-Optical Engineering and Department of Electrical Engineering, National Taiwan University, Taipei 10617, Taiwan, Republic of China
(Received 17 February 2004; revised manuscript received 4 June 2004; published 19 August 2004)

We observed ultrafast electron distribution modulation following the strain oscillation of coherent acoustic nanowaves up to a THz frequency range. Through piezoelectric effects, the acoustic nanowave modifies the electronic subband structure, and further modulates the energy distributions of electrons and holes. With amplitude-fixed acoustic waves, a pronounced enhancement of transmission modulation due to acoustic modulation of electron distribution was observed when the optically probed energy position is close to the Fermi level.

DOI: 10.1103/PhysRevB.70.073307 PACS number(s): 72.50+b, 62.25.+g, 63.22.+m, 78.47.+p

Dynamic control of electronic systems using acoustic waves has made great progress in recent years.[1–3] Several applications of electronic or optoelectronic devices driven by surface acoustic waves (SAWs) have been demonstrated including SAW-induced carrier transport in quantum wires,[1] dynamic band-structure modulation of quantum wells,[2] and dynamic storage of light in quantum wells.[3] However, the wavelength of SAWs in these studies was longer than a few microns, the corresponding modulation frequency was thus in the range of ~100MHz to 4GHz. Restricted by the long acoustic wavelength and the relatively low operation frequency, these demonstrated SAW devices thus have limited operation speed and spatial selectivity.

Laser induced coherent acoustic phonons in solids[4–19] are with frequency up to THz range. A thermal based superconductor bolometer was widely used to detect the energy of the generated coherent or incoherent acoustic phonons,[4–8] with a relatively poor temporal resolution. Taking advantage of time resolution provided by femtosecond optical pulses, the phase oscillations of the THz coherent acoustic phonon were previously resolved through various pump-probe techniques.[9–19] We previously demonstrated the generation of huge coherent LA phonons in piezoelectric semiconductor MQWs and the optically detected oscillation signal was greatly enhanced due to piezoelectric coupling mechanism,[18–23] while the experiments can be performed at room temperature with much lower excitation power. Because the induced LA phonon has a high degree of coherence in time, its generation and propagation can be modeled by a macroscopic continuum elastic theory.[22,23] This semi-classical viewpoint of coherent LA phonon oscillation as an acoustic nanowave (or nanoacoustic wave, NAW) is valid in the coherent regime in which thermal and quantum fluctuations can be neglected. Analogous to an interdigital transducer, in which electric pulses change the electric field in a piezoelectric material to generate SAWs with wavelength determined by the electrode interval,[24] ultrashort optical pulses can excite carriers that screen the electric field in the piezoelectric quantum wells to induce coherent acoustic waves. Through the transient transmission modulation of an ultrashort optical pulse due to quantum confined Franz Keldysh (QCFK) effect, the MQW can also be utilized to detect the propagating coherent acoustic wave,[19,25] This technology resembles the principle of a typical transducer nowadays, however, the acoustic wavelength determined by the period of the MQW can be smaller than 10 nm. Therefore, the MQW structure based on piezoelectric materials is a suitable candidate for ultrahigh bandwidth transducers to generate coherent NAWs with a nanometer wavelength and a THz frequency.

In this report, we demonstrate that NAWs can be applied to control electronic devices through piezoelectric effect with a speed up to the THz range. We treat an InGaN/GaN piezoelectric MQW as an acoustic transducer and generate NAWs with a femtosecond optical pulse. After the NAWs left the MQWs, propagated in the cap layer, reflected at the interface, and returned back into the piezoelectric MQW with a 35–55 ps time-delay, the NAWs are found to modify the electronic subband structure of the MQW according to its phase oscillation, resulting in THz carrier distribution modulation. This observation was confirmed by treating the same InGaN/GaN piezoelectric MQWs as a carrier-populated electronic device and studying the carrier distribution modulation under the presence of the echoed NAW. By probing with different wavelength light and by controlling the carrier population, we confirm that the carriers follow the band modulation with a time scale less than the period of NAW. This observed THz frequency carrier modulation indicates the possibility to apply NAW for the ultra-high speed electronic control in piezoelectric-semiconductor-based quantum devices, with potentially a much higher spatial accuracy due to the much shorter acoustic wavelength.

We used a 14-period 50 Å/43 Å $In_{0.1}Ga_{0.9}N/GaN$ MQW sample[26] as our experimental acoustic transducer, which was grown on a 2.2 μm-thick Si-doped GaN thin film and capped with a 0.1 μm $Al_{0.1}Ga_{0.9}N$ layer. Because of the large piezoelectric constant along the [0001] orientation in group III nitrides, a strain-induced piezoelectric field on the order of MV/cm inside the well region is expected. A room temperature absorption spectrum indicated that the bandgap of the MQW is ~2.92 eV . The UV pulse applied in the experiment was with a pulsewidth of 180 fs, while its central frequency was between 370 and 390 nm with FWHM of ~4 nm. We

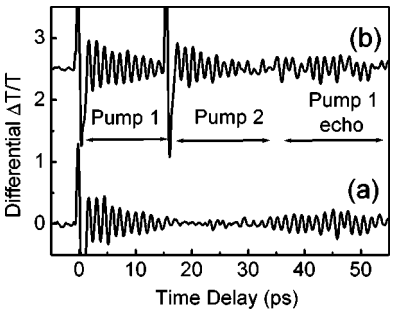

FIG. 1. Measured differentiated probe transmission changes versus probe delay (a) without and (b) with injecting excess carriers by Pump-2 at ~16 ps. The probe photon energy is 3.35 eV.

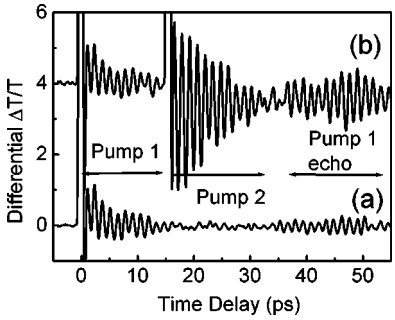

FIG. 2. Measured differentiated probe transmission changes versus probe delay (a) without and (b) with injecting excess carriers by Pump-2 at ~16 ps. The probe photon energy is 3.17 eV.

first used a femtosecond UV pump pulse to excite NAWs in the MQW. The initiated NAWs traveled in two counter-propagation directions, one toward the GaN layer (2.2 μm) and the other toward the cap layer (0.1 μm). Due to the total internal reflection at the cap-air interface, the NAW propagating into the 0.1-μm-thick cap layer will be reflected at the cap-air interface and travel back into the MQW again. We then treated the piezoelectric MQW as a carrier populated electronic device, of which the spatial periodicity matches the acoustic wavelength of the incoming NAW, and studied the possible carrier distribution modulation (CDM) under the presence of the echoed THz frequency NAW. We performed both probe-wavelength and carrier-density dependent transient transmission studies to investigate the interaction between the carrier population and NAWs. In order to control the echoed NAW intensity and carrier density as two independent variables, we fixed the power of the first pump pulse (called Pump-1) to generate fixed amplitude NAW. To control the carrier population inside the MQW before the echoed NAW reentered, we injected excess carriers using an extra femtosecond UV pulse (called Pump-2) after the studied NAW left the MQW region but before the echo reentered. Although Pump-2 also initiated another NAW (called NAW-2), we selected the proper injection time so that the studied NAW reentered into the MQW while NAW-2 was in the cap layer. We then investigated the absorption modulation induced by the fixed amplitude NAW with different carrier concentrations in the MQW. All experiments were performed at room temperature.

Figure 1(a) shows the differentiated probe transmission change as a function of time delay relative to Pump-1 without Pump-2. The signal was differentiated for easier studies of NAW oscillations with a frequency of 0.72 THz.[27] The average power of the incident Pump-1 was 3.7 mW with a corresponding optical fluence of 4.8×10^{-5} J/cm^2. By measuring the reflected and transmitted powers before and after the sample, the Pump-1-induced 2D carrier density per well was estimated to be 4×10^{12} cm^{-2} with a measured focal beam diameter of 11 μm. The pump/probe photon energy was 3.35 eV (370 nm), of which the corresponding transition position was far from the quasi-Fermi level of the generated photocarriers after thermalization estimated by a $\mathbf{k}\cdot\mathbf{p}$ method.[20,28] Note that since the photocarriers relax to quasi-equilibrium with a time constant less than 1 ps,[29,30] as a result, when the echo pulse came back to MQW (after >20 ps), the carriers can be assumed to be in Fermi distribution at room temperature. From the trace (a), we can observe that the initiated NAW completely left the MQW region after ~16 ps, corresponding to the acoustic traveling time across the MQW region, and the echo from the cap layer side starts to reenter the MQW at ~35 ps. Figure 1(b) shows the measured differential transient transmission result with the Pump-2 applied for increasing the carrier density in the MQW. The fluences of Pump-1 for both (a) and (b) cases were kept the same. The optical fluence of pump 2 was $\sim4.8\times10^{-5}$ J/cm^2, which induced an extra 2D carrier density of 4×10^{12} cm^{-2}, resulting in a total carrier density of 8×10^{12} cm^{-2}. We injected extra carriers with Pump-2 at 16 ps while the studied NAW was in the cap layer, and investigated the probe oscillation variation induced by the echo of the studied NAW while NAW-2 was in the cap layer. By comparing trace (b) with trace (a) in Fig. 1, our studied results reveal that the 3.35 eV-probed optical oscillation magnitude, induced by the echo of a fixed-amplitude NAW, remains unchanged as the carrier concentration in the MQW doubles. This study also indicates that after thermalization, the change of the electron-hole wavefunction overlap, which will also modify the optical absorption strength because of the enhanced electric field screening with an increased carrier concentration, is negligible under our experimental condition.

However, by lowering the photon energy down to 3.17 eV (390 nm), the probed optical transition was close to the quasi-Fermi level of the total injected photocarriers after thermalization and was thus sensitive to the possible THz acoustic modulation of the carrier distribution. Figure 2 shows the differentiated probe transmission changes as a function of time delay without [Fig. 2(a)] and with [Fig. 2(b)] Pump-2 with a pump/probe photon energy of 3.17 eV. The optical fluences of Pump-1 were again kept the same ($\sim1.3\times10^{-4}$ J/cm^2), and photocarriers with 2D densities of 9.0×10^{12} cm^{-2} were generated at zero time-delay. The Pump-2 (optical fluence $\sim2.0\times10^{-4}$ J/cm^2) entered the sample at approximately the same time delay (~16 ps) as trace (b) in Fig. 1 and extra photocarriers with a 2D density of 1.2×10^{13} cm^{-2} were injected, resulting in a total 2D concentration of 2.1×10^{13} cm^{-2}. Although the Pump-1-induced NAWs have the same amplitudes for both traces of Figs. 2(a) and 2(b), the returned echo causes a much higher optical

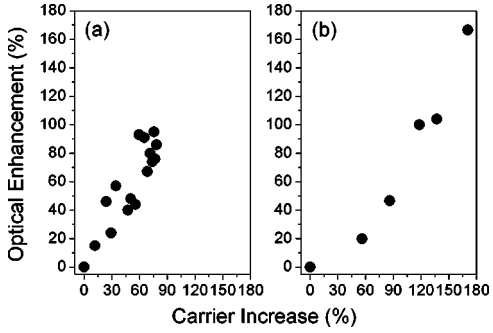

FIG. 3. Probe modulation enhancement versus carrier increase. The initial 2D carrier concentrations were (a) 1.35×10^{13} cm^{-2} and (b) 0.69×10^{13} cm^{-2}. The enhancement is set as 0 without Pump-2 to inject excess carriers. The probe photon energy is 3.17 eV.

transmission modulation with increased background carrier population (called "CDM enhancement"). It is amazing to observe such a high frequency modulation ($\sim$THz) of the carrier population distribution due to NAW.

To further study the relation between the carrier concentration (or quasi-Fermi level) and the NAW-induced probe transmission modulation amplitude, we repeated the experiment in Fig. 2 and varied the power of Pump-2. The measured enhancement of the transmission modulation is plotted versus carrier increase in Figs. 3(a) and 3(b). The initial 2D concentrations were 1.35×10^{13} cm^{-2} and 0.69×10^{13} cm^{-2} for (a) and (b). The differentiated transmission changes in the echo region (39–53 ps) of the traces with different carrier increases were Fourier transformed. The enhancement was then determined according to the optical modulation amplitudes at the oscillation frequency (0.72 THz) in the Fourier spectra. Figure 3 shows that the optical enhancement increases with increasing carriers with a probe photon energy of 3.17 eV.

The THz CDM enhancement of the observed optical modulation can be explained by ultrafast modulation of carrier distribution in piezoelectric MQW due to the incoming THz NAW. Optical absorption in semiconductors under the presence of carriers can be simply described as $\alpha=\alpha_0(1-f_e-f_h)$,[31] where α_0 is the absorption constant without considering Pauli exclusion principle, f_e is the electron distribution, and f_h is the hole distribution. The variation of absorption can be derived as

$$\Delta\alpha = \Delta\alpha_0(1-f_e-f_h) + \alpha_0(-\Delta f_e - \Delta f_h) = \Delta\alpha_{QCFK} + \Delta\alpha_{CDM}. \tag{1}$$

The first term on the right hand side represents the variation of absorption constant α_0. Under the presence of coherent longitudinal NAWs, $\Delta\alpha_0$ was modulated through the QCFK effect at the acoustic frequency due to strain and piezoelectric field modulations. Our study in Fig. 1 indicates that the modulation of absorption constant is not strongly affected by the increased carrier population under our experimental condition, and thus is not responsible for the observed enhancement phenomenon.

On the other hand, strain and piezoelectric field modulations also result in the quantization energy oscillation of the piezoelectric MQW at the acoustic frequency. Our observed strong enhancement effect as shown in Figs. 2 and 3 implies that the carriers can follow the THz-modulated quantization energy. This ultrafast carrier population modulation due to the NAW can thus enhance the total modulation amplitude of optical transmission as reflected in the second term on the right side of Eq. (1), when the probing position is close to the carrier population. In Fig. 1, the probed energy position is far from the Fermi surface, the acoustic wave-induced variation of carrier concentration at the probe energy is so small that $\Delta\alpha_{CDM}$ can be neglected.

Through electron-phonon interactions, the NAW produces an instantaneous modulation of carrier single-particle energy. For the case of ideal parabolic subband, this modulation is due to the instantaneous shift of the quantized band-edge energies, ΔE_c and ΔE_v, for electrons and holes, respectively. For an incident probe photon with energy E_{pr}, there corresponds a resonant in-plane wave vector k_r obtained from energy and momentum conservation. The shift of band-edges results in a shift of resonant wave vector Δk_r which is related to energy shifts as $\Delta k_r=(m_{e,h}/\hbar k_r)\Delta E_{e,h}$, where $m_{e,h}$ is the effective mass of electron and hole, respectively. Assuming that the carriers adiabatically follow the band-modulation, we obtain the following expression for transmission changes due to CDM:

$$\left(\frac{\Delta T}{T}\right)_{\mathrm{CDM}} \propto -\alpha_0(\Delta f_e(E_{pr}) + \Delta f_h(E_{pr})) \propto -\Delta E_c \left.\frac{df_e}{dE}\right|_{E=E_{pr}} - \Delta E_v \left.\frac{df_h}{dE}\right|_{E=E_{pr}}. \tag{2}$$

With a small and fixed oscillation amplitude ΔE_c or ΔE_v of the quantized energy level (determined by NAW amplitude), the amplitude of the probe transmission oscillation can be found to be proportional to the slope of the electron and hole Fermi distributions at the probed energy positions. Since the effective mass of the electron is much lighter than that of the hole, i.e., the Fermi energy shift of the hole distribution is comparatively insensitive to the increasing population in the well, the observed CDM enhancement should be primary from the modulation of the electron population.

From Eqs. (1) and (2), the slope of the electron Fermi distribution partially determines the optical modulation signal with different background carriers in the MQWs. With a higher Fermi level (or higher carrier concentration), the value of $(df_e/dE)_{E=E_{pr}}$ increases and the optical signal thus is enhanced as shown in Fig. 3. The quasi-linear behavior in the case of (a) shows the Fermi level does not shift seriously. But for the case of (b), higher increased carrier population causes the enhancement behavior to deviate from the linear regime.

In summary, we observed ultrafast carrier distribution modulation up to a THz frequency by NAW in a piezoelectric InGaN/GaN MQW. Under the presence of the coherent longitudinal NAW, the quantization energy of the piezoelectric MQW oscillates at the $\sim$ THz acoustic frequency due to strain and piezoelectric field modulations. The carriers in the wells follow the THz quantized-level shift and enhance our observed optical modulation when the probed transition is

close to the Fermi energy. This THz electron distribution modulation in piezoelectric InGaN/GaN MQW due to NAWs confirms the possibility to apply NAWs for the ultrahigh speed electronic control with high spatial accuracy. By using NAWs, the acousto-electronic control will no longer be restricted on the surface while current limitations on the operation speed and spatial selectivity can be greatly improved by orders of magnitude.

The authors would like to acknowledge stimulating scientific discussions with C. J. Stanton. The studied sample was kindly provided by S. Keller and S. P. DenBaars of University of California at Santa Barbara. This work was sponsored by National Science Council of Taiwan, R.O.C. under Grant No. NSC93-2120-M-002-004 and No. NSC92-2112-M-002-044. K.-H. Lin would like to thank SiS Education Foundation for financial support.

*Corresponding author. Email address: sun@cc.ee.ntu.edu.tw

[1] F. Alsina, P. V. Santos, H.-P. Schonherr, W. Seidel, K. H. Ploog, and R. Notzel, Phys. Rev. B **66**, 165330 (2002).
[2] T. Sogawa, P. V. Santos, S. K. Zhang, S. Eshlaghi, A. D. Wieck, and K. H. Ploog, Phys. Rev. B **63**, 121307 (2001).
[3] C. Rocke, S. Zimmermann, A. Wixforth, J. P. Kotthaus, G. Böhm, and G. Weimann, Phys. Rev. Lett. **78**, 4099 (1997).
[4] B. Taylor, H. J. Maris, and C. Elbaum, Phys. Rev. Lett. **23**, 416 (1969).
[5] V. Narayanamurti, H. L. Störmer, M. A. Chin, A. C. Gossard, and W. Wiegmann, Phys. Rev. Lett. **43**, 2012 (1979).
[6] R. G. Ulbrich, V. Narayanamurti, and M. A. Chin, Phys. Rev. Lett. **45**, 1432 (1980).
[7] G. A. Northrop, S. E. Hebboul, and J. P. Wolfe, Phys. Rev. Lett. **55**, 95 (1985).
[8] A. J. Kent, N. M. Stanton, L. J. Challis, and M. Henini, Appl. Phys. Lett. **81**, 3497 (2002).
[9] C. Thomsen, J. Strait, Z. Vardeny, H. J. Maris, J. Tauc, and J. J. Hauser, Phys. Rev. Lett. **53**, 989 (1984).
[10] O. B. Wright and K. Kawashima, Phys. Rev. Lett. **69**, 1668 (1992).
[11] G. Tas, R. J. Stoner, H. J. Maris, G. W. Rubloff, G. S. Oehrlein, and J. M. Halbout, Appl. Phys. Lett. **61**, 1787 (1993).
[12] A. Yamamoto, T. Mishina, Y. Masumoto, and M. Nakayama, Phys. Rev. Lett. **73**, 740 (1994).
[13] J. J. Baumberg, D. A. Williams, and K. Köhler, Phys. Rev. Lett. **78**, 3358 (1997).
[14] A. H. Chin, R. W. Schoenlein, T. E. Glover, P. Balling, W. P. Leemans, and C. V. Shank, Phys. Rev. Lett. **83**, 336 (1999).
[15] A. Bartels, T. Dekorsy, H. Kurz, and K. Kohler, Phys. Rev. Lett. **82**, 1044 (1999).
[16] A. M. Lindenberg, I. Kang, S. L. Johnson, T. Missalla, P. A. Heimann, Z. Chang, J. Larsson, P. H. Bucksbaum, H. C. Kapteyn, H. A. Padmore, R. W. Lee, J. S. Wark, and R. W. Falcone, Phys. Rev. Lett. **84**, 111 (2000).
[17] H.-Y. Hao and H. J. Maris, Phys. Rev. Lett. **84**, 5556 (2000).
[18] C.-K. Sun, J.-C. Liang, C. J. Stanton, A. Abare, L. C. Coldren, and S. P. DenBaars, Appl. Phys. Lett. **75**, 1249 (1999).
[19] C.-K. Sun, J.-C. Liang, and X.-Y. Yu, Phys. Rev. Lett. **84**, 179 (2000).
[20] G. D. Sanders, C. J. Stanton, and C. S. Kim, Phys. Rev. B **64**, 235316 (2001).
[21] C.-K. Sun, G.-W. Chern, K.-H. Lin, and Y.-K. Huang, Chin. J. Phys. (Taipei) **41**, 643 (2003);
[22] G.-W. Chern, C.-K. Sun, G. D. Sanders, and C. J. Stanton, Top. Appl. Phys. **92**, 339 (2004).
[23] G.-W. Chern, K.-H. Lin, Y.-K. Huang, and C.-K. Sun, Phys. Rev. B **67**, 121303 (2003).
[24] See, for example, D. Royer and E. Dieulesaint, *Elastic Waves in Solids* (Springer, New York, 2000).
[25] G.-W. Chern, K.-H. Lin, and C.-K. Sun, J. Appl. Phys. **95**, 1114 (2004).
[26] S. F. Chichibu, A. C. Abare, M. S. Minsky, S. Keller, S. B. Fleischer, J. E. Bowers, E. Hu, U. K. Mishra, L. A. Coldren, S. P. DenBaars, and T. Sota, Appl. Phys. Lett. **73**, 2006 (1998).
[27] For typical traces of probe transmission changes as a function of time delay, please consult Refs. 18 and 19.
[28] S. L. Chuang and C. S. Chang, Semicond. Sci. Technol. **12**, 252 (1997).
[29] C.-K. Sun, Y.-L. Huang, S. Keller, U. K. Mishra, and S. P. DenBaars, Phys. Rev. B **59**, 13 535 (1999).
[30] C.-K. Sun, F. Vallée, S. Keller, J. E. Bowers, and S. P. DenBaars, Appl. Phys. Lett. **70**, 2004 (1997).
[31] W. H. Knox, in *Hot Carriers in Semiconductor: Nanostructures*, edited by J. Shah (Academic, New York, 1992).